



HAL
open science

New thiosemicarbazone Schiff base ligands: Synthesis, characterization, catecholase study and hemolytic activity

Oussama Kheireddine Nehar, Radia Mahboub, Samira Louhibi, Thierry Roisnel, Mohammed Aissaoui

► To cite this version:

Oussama Kheireddine Nehar, Radia Mahboub, Samira Louhibi, Thierry Roisnel, Mohammed Aissaoui. New thiosemicarbazone Schiff base ligands: Synthesis, characterization, catecholase study and hemolytic activity. *Journal of Molecular Structure*, 2020, 1204, pp.127566. 10.1016/j.molstruc.2019.127566 . hal-02470138

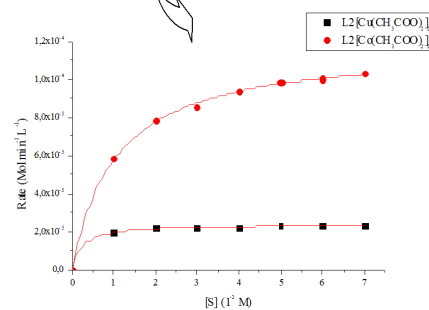
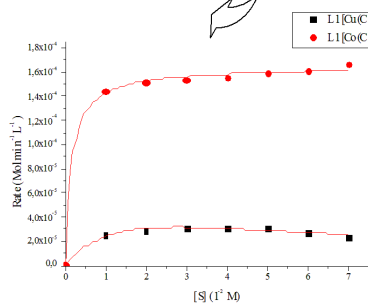
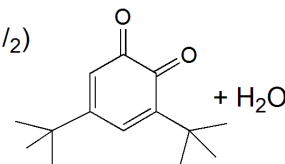
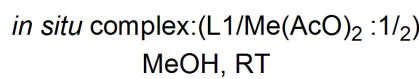
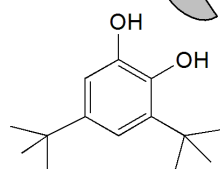
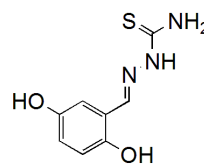
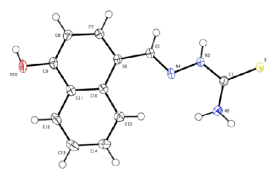
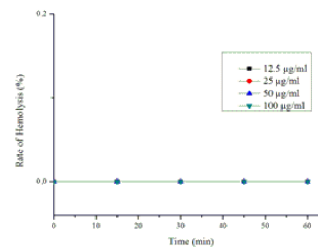
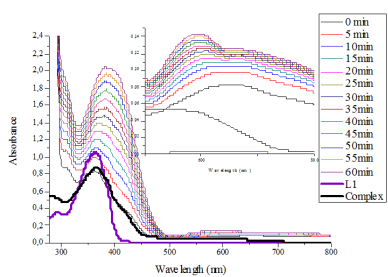
HAL Id: hal-02470138

<https://univ-rennes.hal.science/hal-02470138>

Submitted on 13 Feb 2020

HAL is a multi-disciplinary open access archive for the deposit and dissemination of scientific research documents, whether they are published or not. The documents may come from teaching and research institutions in France or abroad, or from public or private research centers.

L'archive ouverte pluridisciplinaire **HAL**, est destinée au dépôt et à la diffusion de documents scientifiques de niveau recherche, publiés ou non, émanant des établissements d'enseignement et de recherche français ou étrangers, des laboratoires publics ou privés.



New thiosemicarbazone Schiff base ligands: Synthesis, characterization, catecholase study and hemolytic activity

Oussama Kheireddine Nehar¹, Radia Mahboub², Samira Louhibi¹, Thierry Roisnel³ and Mohammed Aissaoui⁴

¹ Laboratory of inorganic chemistry and environment, Departement of Chemistry, Faculty of Science, BP 119, Tlemcen University, Tlemcen 13000, Algeria.

² Department of Chemistry, Faculty of Sciences, University of Tlemcen, B.P. 119, Tlemcen, 13 000, Algeria.
e-mail: radiamahboub@yahoo.com

³ Center of Diffractometry X, UMR 6226 CNRS, University of Rennes 1, 35042 Rennes, France

⁴ Antibiotics Antifungal Laboratory: Physical-Chemistry, Synthesis and Biological Activity, Faculty of Biology, Tlemcen University, Tlemcen 13000, Algeria

Corresponding author*: samhibi1@yahoo.fr

Abstract

Two novel thiosemicarbazones ligands have been synthesized and characterized by FT-IR, ESI-MS, ¹H NMR, and also by single-crystal X-ray diffraction for L1. The crystal structure shows that L1 molecules are planar and are connected via N-H---S and O-H---S interactions. The catecholase activity of *is situ* copper and cobalt complexes of this ligands has been investigated against 3,5-di-tert-butylcatechol. The progress of the oxidation reactions was closely monitored over time following the strong peak of 3,5-DTBC using UV-Vis. Oxidation rates were determined from the initial slope of absorbance vs. time plots, then analyzed by Michaelis-Menten equations. Catechol oxidation reactions were realized using different concentrations of copper and cobalt acetate and ligands (L/Cu: 1/1, 1/2, 2/1). The results show that all complexes were able to catalyze the oxidation of 3,5-DTBC. Acetate complexes have the highest activity. CuL1 and CoL1 complexes act as a catalyst and inhibitor. While copper and cobalt complexes obtained from ligand L2 illustrate concentration-independent oxidation activation. The hemolysis study performed by L1 increases as a function of its concentration. However, ligand L2 has no hemolytic effect.

Keywords: Thiosemicarbazone, Crystal structure, Catechol Oxidation, Catalysis, hemolytic activity.

1. Introduction

Proteins are the most important building blocks of a living cell. They carry out a large variety of functions [1], such as: structural stabilization, molecule transport and catalysis. Metalloproteins are estimated to represent about one third of all proteins [2]. A significant number of them contain transition metal ions such as iron, copper, nickel, zinc and molybdenum [3].

Copper Metalloproteins are very interesting because of their biological activities as catalysts in redox reactions. Studies on copper metalloproteins led to their classification based on spectroscopic features into 3 types: type-1, type-2 and type-3 active sites [4]. Copper proteins with a type-3 active site, have an intriguing ability to reversibly bind dioxygen under ambient conditions [4, 5]. This category of proteins includes catechol oxidase, an enzyme which catalyzes exclusively the oxidation of catechols to the corresponding quinones [6, 7]. In literature, considerable amount of studies are investigated on the synthesis of dicopper compounds in order

to mimic the activity of catechol oxidase. Their catalytic activity has been investigated in the literature as *in situ* [8, 9] or as isolated complexes [5, 10]. In recent years, mononuclear copper complexes also were reported to demonstrate catecholase activity [11]. Nevertheless many other metal complexes are being studied to investigate their catechol oxidase capacities [12–14].

Thiosemicarbazones are one of the main subgroups of hydrazine. They are obtained through the reaction of thiosemicarbazides with aldehydes or ketones. Thiosemicarbazones are a group of compounds with numerous pharmacological applications such as antibacterial [15], antifungal, antiviral [16], anti-inflammatory [17], antituberculosis [18], and antitumoral [19]. The antitumoral activity of these compounds is due to their capacity to restrain ribonucleotide reductase (RR), an enzyme necessary for DNA synthesis [20]. Moreover, their metal complexes possess valuable catalytic activities [21, 22], as well as pharmacological properties as drug candidates, biomarkers and biocatalysts [23, 24]. Thiosemicarbazones are also reported to have various analytical applications [25, 26]. They are used as corrosion inhibitors [27] and as heavy metals in removal wastewater [28].

In the present work, we report the synthesis of two novel thiosemicarbazone Schiff base ligands (L1, L2), their characterizations by spectroscopic methods and by single-crystal X-ray diffraction for L1. Then, we study the catalytic activity of the *in situ* metal-thiosemicarbazone complexes (CuL1, CuL2, CoL1 and CoL2) towards the oxidation of 3,5-di-*tert*-butylcatechol. Finally, we present the hemolytic activity of ligands L1 and L2.

2. Experimental

2.1. Materials and Physical measurements

All the chemicals and solvents were reagent grade, and they were used as purchased with no further purification.

X-ray data were collected on a D8 VENTURE Bruker AXS diffractometer with Mo-K α radiation ($\lambda = 0.71073 \text{ \AA}$). IR spectra were measured in the 400-4000 cm^{-1} range on a 9800 FTIR spectrometer (Perkin–Elmer) where samples were run as KBr pellets. IR spectra were measured in the 400-4000 cm^{-1} range on a Perkin-Elmer spectrum two spectrometer. Samples were run as KBr pellets. ^1H nuclear magnetic resonance spectra were realized using Varian Mercury M400 400 MHz spectrometer. Chemical shifts are listed in ppm and are reported relatively to tetramethylsilane using the acetone- d_6 solvent. Mass spectra were done on a spectrometer LC/MSD-TOF G1969A (ESI-MS). Kinetic measurements were carried on spectrophotometrically using UV-Vis on Perkin Elmer Lambda 25 and OptizenPOP 3 spectrophotometers.

2.2. Synthesis of (*E*)-2-((4-hydroxynaphthalen-1-yl)methylene)hydrazinecarbothioamide L1

In a mixture of three solvents: (water, ethanol and acetic acid) in a ratio of (1:3:3), was dissolved 10 mmol/10ml (1.72 g) of 3-hydroxy-2-naphthaldehyde. Then 10 mmol/10ml (0.91 g) of thiosemicarbazide was added. The mixture was refluxed for 2h and was left to recrystallize at room temperature. After slow evaporation, brown crystals suitable for XRD analysis were formed. Yield: 79%. MP = 256 °C.

^1H NMR (400 MHz, Acetone- d_6), δ (ppm): 7.40 and 7.70 (2H, NH_2), 6.69 and 7.55-8.62 (6H, CH_{Ar}), 8.84 (s, 1H, $=\text{CH}-\text{Ar}$), 9.60 (s, 1H, OH), 10.30 (s, 1H, NH). Selected IR bands (KBr pellet, cm^{-1}): 3420 (OH), 3320a /3200s (NH_2), 3177 (NH), 3030 ($\text{C}-\text{H}_{\text{Ar}}$), 1577 ($\text{C}=\text{C}$), 1511 ($\text{C}=\text{N}$), 1115/ 783 ($\text{C}=\text{S}$), 967 (N-N). MS (ESI) (m/z): $[\text{M}-\text{H}]^+$ 244.05.

2.3. Synthesis of (*E*)-2-(2,5-dihydroxybenzylidene)hydrazinecarbothioamide L2

To an ethanolic solution of thiosemicarbazide 10 mmol/10ml (0.91 g), was added 10 mmol (1.38 g) of 2,5-dihydroxybenzaldehyde dissolved in 10 ml of ethanol, in the presence of catalytic amount of glacial acetic acid. The mixture then was refluxed for 2h. The obtained precipitate was filtrated, rinsed with ethanol, and left to dry overnight in room temperature. Yield: 86%. MP = 266 °C.

¹H NMR (400 MHz, acetone-d₆) δ (ppm): 6.30-6.84 (m, 2H, H_{ar}), 7.08 (s, 1H, H_{Ar}), 7.44 and 7.68 (s, 2H, NH₂), 7.92 (s, 1H, NH), 8.39 (s, 1H, =CH-Ar), 8.70 (s, 1H, OH) and 10.38 (s, 1H, OH). Selected IR bands (KBr pellet, cm⁻¹): 3432 (OH), 3333a /3145s (NH₂), 3177 (NH), 3030 (C-H_{Ar}), (C=C), 1627 (C=N), 1161/ 797 (C=S), 943 (N-N). MS (ESI) (*m/z*): [M-H]⁺ 210.03.

2.4. X-ray crystallography

The data of single crystal L1 were collected on D8 VENTURE Bruker AXS diffractometer with Mo-K α radiation of wavelength $\lambda = 0.71073$ Å. The ligand L1 crystallizes in the triclinic space group P-1. The molecular structure of L1 is shown in (Figure 2). The cell parameters of L1 as well as the structural data are grouped in Table 1. The structure of L1 was solved by direct methods using the SIR97 program [29] and then refined with full-matrix least-square methods based on F2 (SHELXL-97) [30]. All non-hydrogen atoms were refined with anisotropic atomic displacement parameters. Except, nitrogen and oxygen linked hydrogen atoms that were introduced in the structural model through Fourier difference maps analysis, H atoms were finally included in their calculated positions. A final refinement on F2 with 2560 unique intensities and 166 parameters converged at ωR (F2) = 0.0834 (R(F) = 0.0318) for 2305 observed reflections with $I > 2\sigma(I)$.

2.5. Catecholase activity study

In situ catechol oxidase study was performed in DMF. 3,5-di-tert-butylcatechol (3,5-DTBC) was used as substrate [6, 13]. In a spectrophotometric cell, ligand (L1 and L2) (10^{-4} M) and metal salt (Cu(AcO)₂ and Co(AcO)₂) (10^{-4} M) solutions were mixed together then treated with 100:1 up to 700:1 substrate to complex ratios (1×10^{-2} - 7×10^{-2} M). The progress of oxidation reactions was regularly monitored over time at room temperature, under aerobic conditions. Absorbance values were recorded following the strong peak of 3,5-di-tert-butylquinone (3,5-DTBQ) [7] (400 nm maximum absorbance) using UV-Vis spectroscopy. Oxidation rates were determined from the initial slope of absorbance vs. time plots, and then analyzed by Michaelis-Menten equations (Eq.1, Eq.2).

$$V_0 = \frac{V_{max} \times [S]}{[S] + K_m} \quad (1)$$

$$V_0 = \frac{V_{max} \times [S]}{[S] + K_m \left(1 + \frac{[S]}{K_i}\right)} \quad (2)$$

Were K_i is the inhibition constant, K_m is the Michaelis constant, $[S]$ is the concentration of the substrate, V_0 is the velocity and V_{max} is the maximum velocity.

2.6. In vitro hemolytic activity

From a breast patient, a blood sample was taken on heparin tube and centrifuged at 4000 rpm at 4 ° C for 5 minutes. The pellet was washed twice with NaCl solution (150 mM) and then centrifuged at 4000 rpm at 4 ° C for 5 minutes. Subsequently, the pellet was diluted to 2% in PBS (saline phosphate buffer) at 10 mM, pH 7.4. 2970 μ L of the 2% erythrocyte suspension was

placed in contact with 30 μl of ligand at different concentrations and then incubated in a benchtop incubator (Orbital Shaker Thermo Forma) at 37 ° C. for 60 min. 100 μl was taken every 15 min to be resuspended in 1900 μl of PBS. The tubes are centrifuged at 4000 rpm for 5 min. Leakage of intracellular hemoglobin was measured by reading the absorbance at 548 nm. Total hemolytic was achieved by suspending red blood cells with Triton X-100. The buffer alone was used as a negative control. The hemolytic rate was determined as a percentage by the following equation (Eq.3) [31]:

$$\text{Hemolysis rate (\%)} = [(A_{\text{sample}} - A_{\text{spontaneous hemolysis}}) / (A_{\text{triton X-100}} - A_{\text{spontaneous hemolysis}})] \times 100 \text{ Eq.3}$$

3. Results and discussion

3.1. Synthesis of (*E*)-1-((4-hydroxynaphthalen-1-yl)methylene)thiosemicarbazide (L1)

In this work, we have modified the condensation reaction of thiosemicarbazide with 4-hydroxy-1-naphthaldehyde [32]. So, we have prepared the ligand L1 using a mixture of three solvents: (water, ethanol and acetic acid) in a ratio of (1:3:3). As a result, the use of water and an excess of acetic acid were more advantageous to obtain L1 in crystal form.

The formation of L1 is characterized by the presence of characteristic IR bands. Two main absorption bands of the thionic function (C=S) appeared at 1115 cm^{-1} and 783 cm^{-1} and one band of the azomethine function (C=N) presents at 1616 cm^{-1} . These results are comparable to those of literature [33, 34]. The ligand L1 exists in thione form at solid state which is confirmed by the absence of the (S-H) band in the IR spectra (Figure S1a). In DMSO, the thiol (S-H) band appears around 2570 cm^{-1} (Figure S1b). We have not found this result in literature. Furthermore, ^1H NMR spectrum of L1 in deuterated acetone gives signals at 7.4 ppm (s, 1H) and 7.7 (s, 1H) ppm corresponding to the NH_2 function (Figure S1c). In literature, the ^1H NMR data for the isomer: 1-((2-hydroxynaphthalen-1-yl)methylene)thiosemicarbazide shows that NH_2 protons are observed at 7.82 ppm [35]. These chemical shifts depend both on the position of hydroxyl group on the aromatic rings and the used solvents.

3.2. Crystal Structure of ligand L1

The molecular structure of L1 is illustrated in Figure 1. The main crystal parameters are reported in Table 1. The ligand L1 crystallizes with two molecules per unit cell. The sulfur and nitrogen imine (N4) atoms are in *trans*-position with respect to the C1-N3 bond. This result is in agreement with the literature [36-38]. The molecule shows an (*E*) conformation with respect to the C5=N4 bond and is approximately planar. The maximum deviation from the mean plane through the 18 non-hydrogen atoms is 0.118 (2) Å for C5. This planarity is due to electron delocalization along the skeleton of the molecule. In Table 2, we give the selected interatomic distances and angle values. So, these bond lengths and angles agree very well with those observed for similar thiosemicarbazones [39]. In the crystal, the stacking of molecules is in a zigzag shape along the b axis (Figure 2). The three-dimensional network is established by short oxygen-sulfur contacts ($d(\text{O}\cdots\text{S}) = 3.195 \text{ \AA}$) and three types hydrogen bonds ($\text{S}_1\cdots\text{H}_{10}$, $\text{S}_1\cdots\text{H}_3$ and $\text{S}_1\cdots\text{H}_{2B}$) shown in Figure 2 (red color). These parameters are grouped in Table 3. Within this network, there are also van der Waals interactions ($\text{C}_{\text{Ar}}\text{-H}_{12}\cdots\text{H}_{12}\text{-C}_{\text{Ar}}$) and $\text{CH}\cdots\pi$ interactions ($\text{N}=\text{HC}_5\cdots\text{C}_{16}\text{-Ar}$) involving the symmetry-related naphthalene rings. Their respective distances are 2.227 Å and 3.282 Å (blue color in Figure 2).

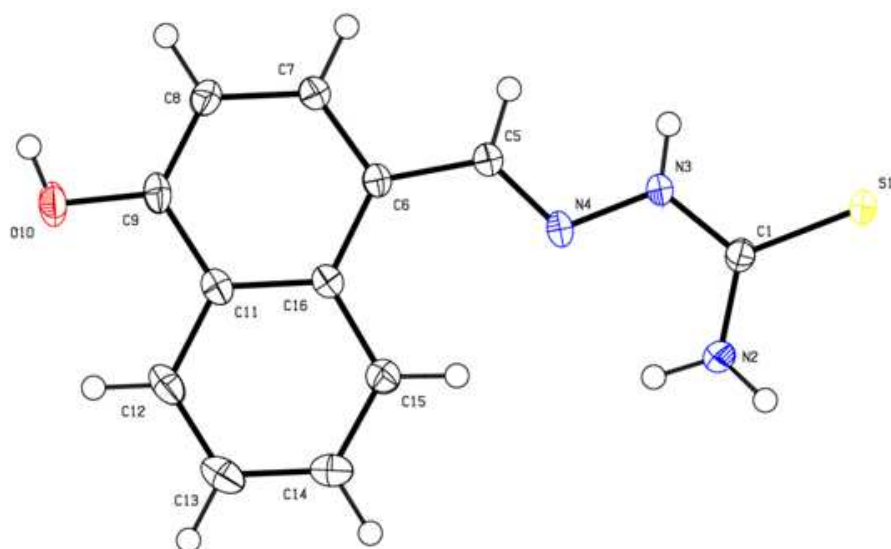


Figure 1. ORTEP representation of ligand L1 with 50% thermal ellipsoid plot; T=150K.

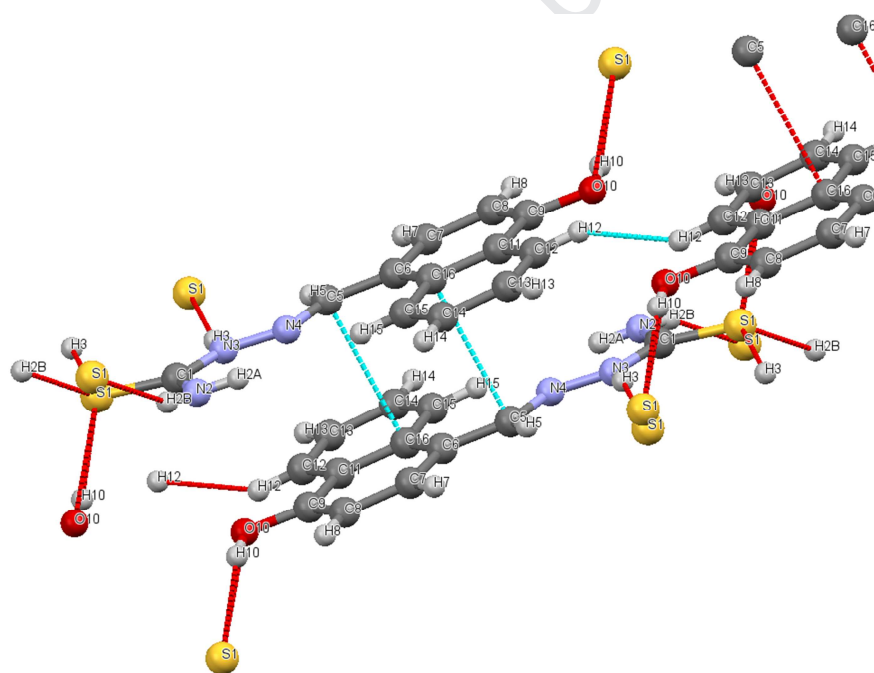


Figure 2. Packing and projection of L1 along the b axis showing S---O contacts, hydrogen bonds and C-H... π interactions.

Table 1 Crystallographic parameters of L1.

Crystal data	L1
Chemical formula	$C_{12}H_{11}N_3OS$
M_r	245.30
Crystal size (mm)	0.440 x 0.260 x 0.200
Crystal system	Triclinic

Space group	P-1
<i>Unit cell parameters</i>	
a	6.8023 (Å)
b	8.4470 (Å)
c	11.1599 (Å)
Z	2
α (deg)	93.353
β (deg)	105.959
γ (deg)	111.749
V (Å ³)	563.33
D _{calc} (g cm ⁻³)	1.446
T (K)	150
μ (mm ⁻¹)	0.273
F(000)	256
R(int)	0.0329
Total reflections	9529
Unique reflections	2560
I>2 σ	2305
Number of parameters	166
R ₁	0.0318
wR ₂	0.0834
Goodness-of-fit (GOF)	0.970

Table 2 Bonds and angles parameters of L1.

Selected bonds (Å)		Selected angles (°)	
C9 - O10	1.3555(15)	N3- C1-S1	119.78(10)
O10 - H10	0.82(2)	N2- C1-S1	122.93(10)
C15 - H15	0.9500	N2- C1-N3	117.29(12)
C6 - C7	1.3825(17)	C5- N4-N3	114.58(11)
C5 - C6	1.4556(17)	N4- C5- C6	125.48(11)
N4 - C5	1.2872(17)	C15-C16-C6	123.53(11)
N3 - N4	1.3835(14)	C14- C15-C16	120.78(12)
N3 - H3	0.850(18)	C9- O10- H10	106.2(14)
C1 - N3	1.3389(16)	-	-
C1 - N2	1.3325(17)	-	-
C1 - S1	1.7006(13)	-	-

Table 3 Hydrogen bonds of L1.

Entry	Hydrogen bonds	Distances (Å)			Symmetry
		D-H...A	d(H...A)	d(D-H)	
1	O ₁₀ -H ₁₀ ...S ₁	2.418	0.820(2)	3.195	-1+x,y,z
2	N ₂ -H _{2B} ...S ₁	2.696	0.845(19)	-	-1+x,y,z
3	N ₃ -H ₃ ...S ₁	2.617	0.850(18)	-	-1+x,y,z

3.3. Synthesis of (*E*)-1-(2,5-dihydroxy benzylidene)thiosemicarbazide (L2)

The ligand L2 was prepared by condensation of thiosemicarbazide with 2,5-dihydroxybenzaldehyde in ethanol. The formation of L2 is characterized by the presence of characterized IR bands. Two main absorption bands of the thionic function (C=S) appeared at 1161 cm⁻¹ and at 797 cm⁻¹ and one band of the azomethine function (C=N) presents at 1627 cm⁻¹. These results are comparable to those of literature [33, 34]. Ligand L1 exists in thione form at

solid state (Figure S2a). While the presence of the (S-H) band in the IR spectra appears around 2570 cm^{-1} in DMSO solution (Figure S2b). To our knowledge, this result has not been reported in literature. In addition, ^1H NMR spectrum of L2 in deuterated acetone shows signals at: 7.75 ppm (s, 1H) and at 7.4 (s, 1H) ppm corresponding to the NH_2 function (Figure S2c). In literature, the ^1H NMR data for the isomer: 1-(2,4-dihydroxybenzylidene)thiosemicarbazide shows that NH_2 protons are observed at 9.82 ppm [40]. These chemical shifts depend both on the position of hydroxyl group on the aromatic rings and the used solvents.

4. Catecholase activities

4.1. UV-Visible studies of the ligands L1 and L2

UV-Vis spectra of L1 show two bands: first at 295 nm corresponding to $n \rightarrow \pi$ transition in the thiosemicarbazone group, and second one at 365 nm corresponding to $\pi \rightarrow \pi$ transition of the naphthalene ring (Fig 3a).

UV-Vis spectra of L2 show two bands: first at 313 nm corresponding to $n \rightarrow \pi$ transition in the thiosemicarbazone group and second at 360 nm corresponding to $\pi \rightarrow \pi$ transition of the benzyl ring (Fig 3b).

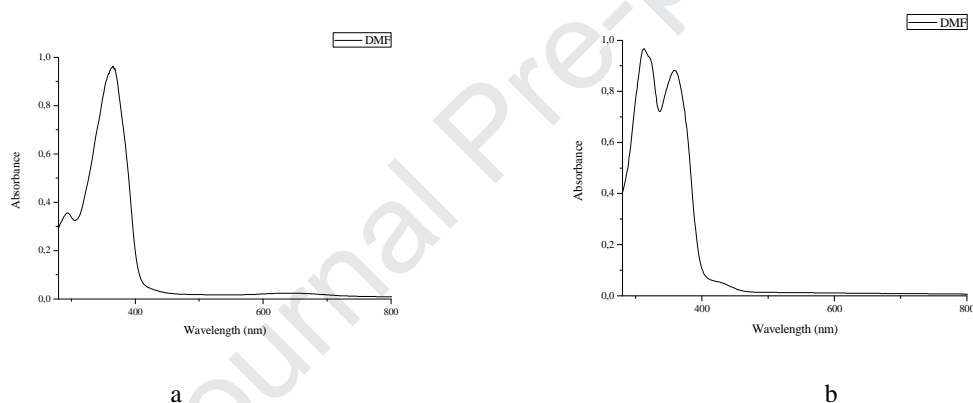


Figure 3: UV-Vis spectra of: a) ligand L1 and b) ligand L2 at 400-800 nm in DMF.

4.2. Effect of ligands concentration on the catecholase activity

The formation of the *in situ* complexes of copper and cobalt ions was followed by the measurement of UV-visible absorption at room temperature in DMF. In order to study the influence of ligand concentration to obtain the best *in situ* catalysts during the oxidation reaction of 3,5-DTBC to 3,5-DTBQ, we have realized this reaction using different concentration of ligand (L1 and L2) and metal ion (Cu and Co) (L/M: 1/1; 2/1; 1/2).

From the results obtained in Figure 6, we note that the combination of 2 moles of metal and 1 mole of ligand leads to an excellent result. Therefore, we consider that the proportion (L/M: 1/2) is a catalytic condition of choice for this reaction.

However, we note a particular situation in the combination of cobalt with ligands. For ligand L1, the combinations (L1/Co: 1/2) and (L1/Co: 1/1) are similar (Figure 4c). We think that this specificity is related to the nature and the characteristic of cobalt and may be due to the coordinating environment.

Based on these results, we can suggest that the oxidation reaction occurs with two metal ions associated with one ligand molecule.

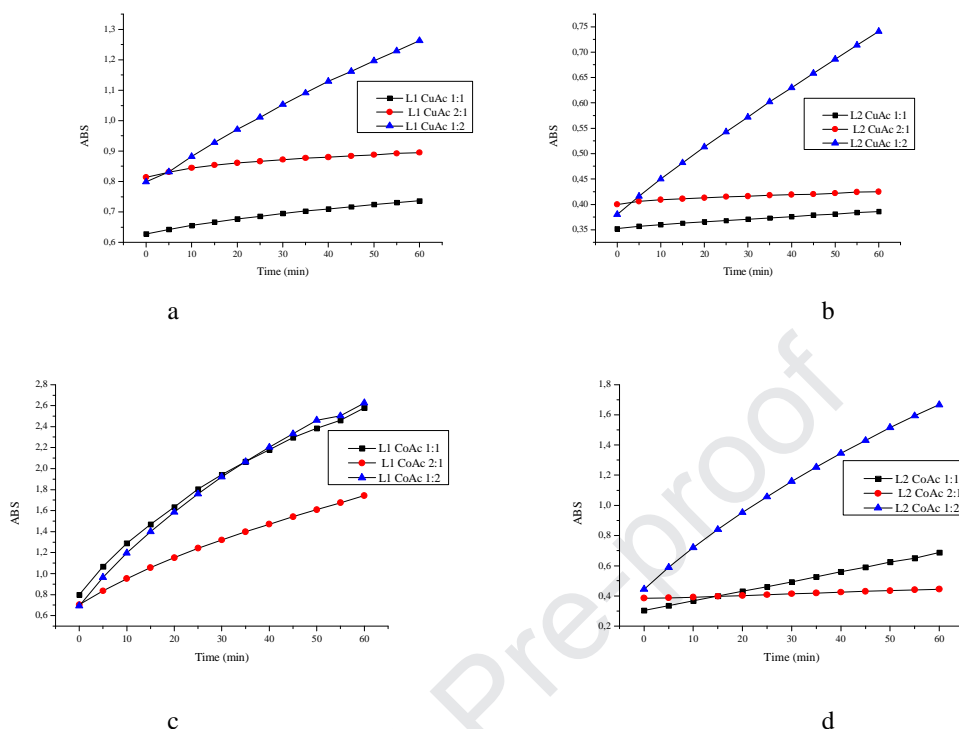


Figure 4: Oxidation of 3,5-DTBC with different concentration of copper acetate and ligands. a) L1Cu, b) L2Cu, c) L1Co and d) L2Co.

4.3. UV-Visible studies of the *in situ* complexes

UV-Vis survey scans were carried out at room temperature in DMF. UV-Vis spectra of *in situ* copper complexes (Cu/L1: 2/1) show different bands (Figure 5a). First band at 295 nm corresponds to $n \rightarrow \pi$ transition of the thiosemicarbazide group. Second one at 365 nm corresponds to $\pi \rightarrow \pi$ transition of the naphthalene ring. In the course of complexation, we note a hypsochromic effect of the band at 280 nm of the thiosemicarbazide group and bathochromic effect of the band at 380 nm of the naphthalene ring. The appearance of two bands, one at 400 nm and the other at 620 nm is attributed to d-d transition which can suggest two geometries: square plane and square pyramidal respectively (Scheme 1a) [41]. In the case of *in situ* cobalt complexes (Co/L1: 2/1), hypsochromic and bathochromic effects are not appearance (Figure 5b). The presence of two bands at 530 nm and 580 nm are attributed to d-d transition that suggests a pseudo-octahedral geometry (Scheme 1b) [42]. Thus, the cobalt charge is Co^{+3} because of its oxidation with air oxygen.

UV-Vis spectra of *in situ* copper complexes (Cu/L2: 2/1) show different bands (Figure 5c). The band at 315 nm corresponds to $n \rightarrow \pi$ transition of the thiosemicarbazide group. Another one at 360 nm corresponds to $\pi \rightarrow \pi$ transition of the benzene ring. During complexation, we note a bathochromic effect of the two bands of thiosemicarbazide group and benzyl group at 330 nm and 420 nm respectively. The bands at 410 nm and at 610 nm are attributed to d-d transition suggesting square plane and square pyramidal geometries respectively (Scheme 1c) [43]. In the case of *in situ* cobalt complexes (Co/L2: 2/1), the hypsochromic effect appears of benzyl and thiosemicarbazide groups at 265 nm and 345 nm respectively (Figure 5d). The two bands at 430

nm and 600 nm are attributed to d-d transition that suggests a distorted octahedral geometry (Scheme 1d) [44]. Similarly, the cobalt charge is Co^{+3} because of its oxidation with air oxygen.

In addition, by comparing the results given in Fig.5, we note that the characteristics of the *in situ* copper(II) and cobalt(III) complexes are similar to those found in the literature [45]. Thus, we propose complex structures obtained during the oxidation process. The complex structures are given in Scheme 1.

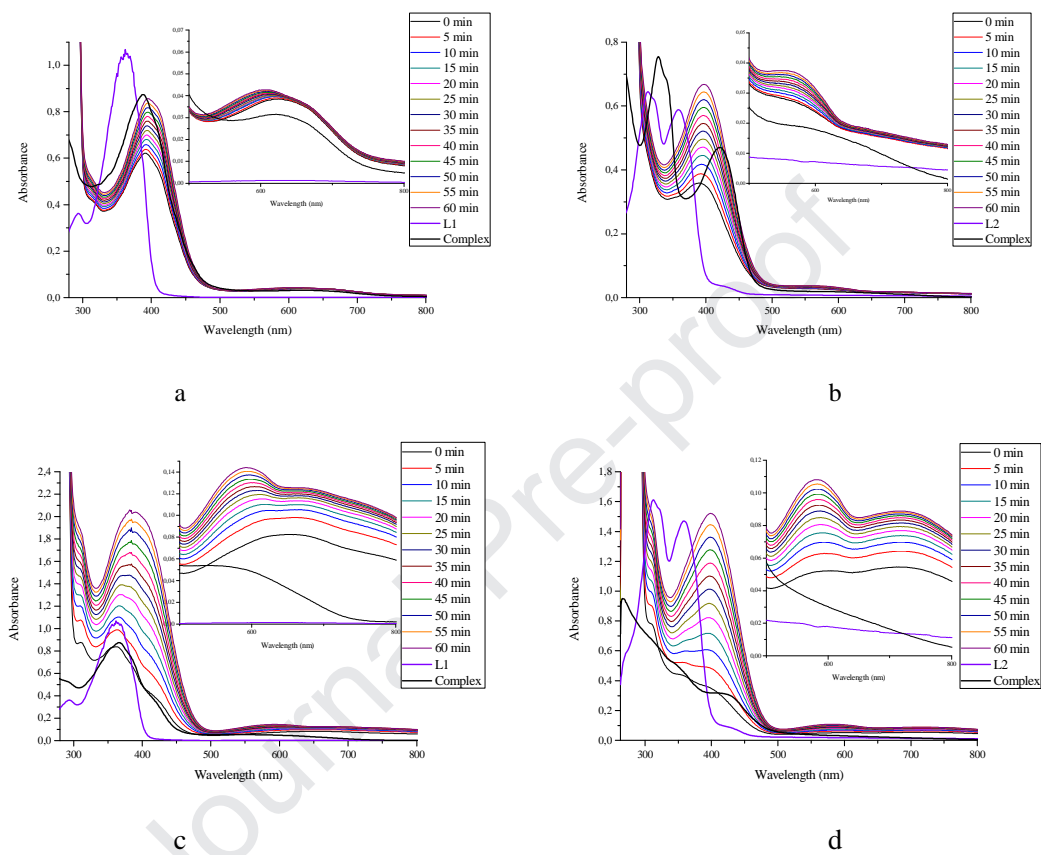
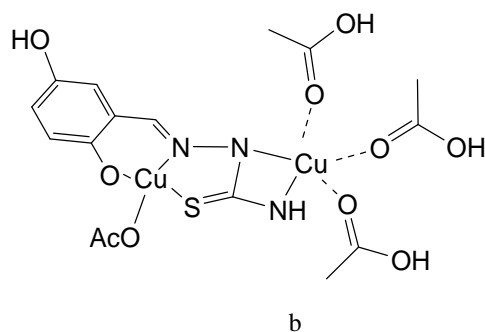
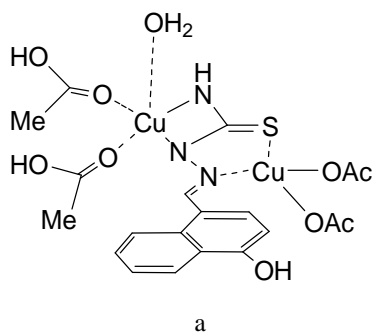
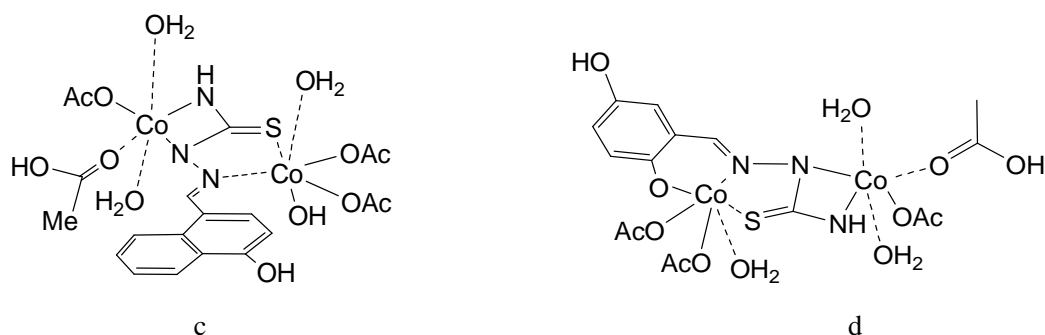


Figure 5: UV/Vis analysis of the 3,5-DTBC oxidation by *in situ* complexes obtained with 1/2 ligand/copper (II) acetate combination over time. a) L1Cu, b) L2Cu, c) L1Co and d) L2Co.





Scheme 1. Proposed structures for the *in situ* complexes (Me/L: 2/1). a) $2\text{Cu}(\text{AcO})_2 \cdot \text{L1} \cdot \text{H}_2\text{O}$, b) $2\text{Cu}(\text{AcO})_2 \cdot \text{L2}$, c) $2\text{Co}(\text{OH})(\text{AcO})_2 \cdot \text{L1} \cdot 2\text{H}_2\text{O}$ and d) $2\text{Co}(\text{OH})(\text{AcO})_2 \cdot \text{L2} \cdot \text{H}_2\text{O}$.

4.4. Michaelis-Menten kinetics

4.4.1. Oxidation reactions using *in situ* copper complexes (L1Cu and L2Cu)

Catechol oxidation reactions were realized using different concentration of copper acetate and ligands (L/Cu: 1/1, 1/2, 2/1). In Figures 6, we give the absorbance of 3,5-DTBC for each proportion. According to the results given in Table 4, we note that the combination obtained by 2 moles of copper and one mole of each ligand gives the best catalytic condition for the oxidation reaction of 3,5-DTBC (Table 4, entries 2 and 5).

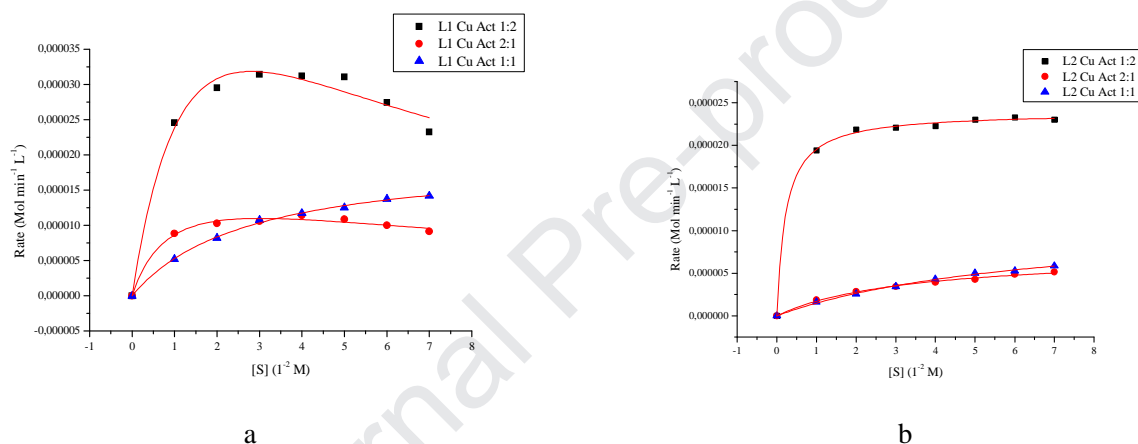
For ligand L1, we note that the kinetic models of two *in situ* copper complexes (L1/Cu: 1/2 and L1/Cu: 2/1) follow the model of enzyme inhibition by excess of substrate. Thus, the complexes exhibit an increase in activity as the concentration increases but beyond a certain concentration of substrate. At the concentration $4 \cdot 10^{-2}$ M of (L1/Cu: 1/2), the activity decreases due the inhibition effect caused by the excess of substrate by applying the modified Michaelis-Menten model (Equ.2) while the *in situ* complex (L1/Cu: 1/1) follow the simple Michaelis-Menten model (Equ.1) (Figure 8a). The complex obtained from copper (II) acetate (L1/Cu: 1/2) shows highest activity (Table 4, entry 2, $V_{\max} = 7.57 \times 10^{-5} \text{ mol. L}^{-1} \cdot \text{min}^{-1}$, $K_{\text{cat}} = 45.42 \text{ h}^{-1}$) if compared to those of proportions: (L1/Cu: 1/1) (Table 4, entry 1, $V_{\max} = 1.98 \times 10^{-5} \text{ mol. L}^{-1} \cdot \text{min}^{-1}$, $K_{\text{cat}} = 11.90 \text{ h}^{-1}$) and (L1/Cu: 2/1) (Table 4, entry 3, $V_{\max} = 1.82 \times 10^{-5} \text{ mol. L}^{-1} \cdot \text{min}^{-1}$, $K_{\text{cat}} = 10.92 \text{ h}^{-1}$) (Figure 6a). To our knowledge, this study has not been reported in literature.

For ligand L2, we note that the kinetic models of different *in situ* copper complexes follow the simple Michaelis-Menten equation (Eq. 1). The kinetic parameters reveal that the complex obtained from 2 moles of copper (II) acetate and one mole of ligand L2 exhibits the highest activity (Table 4, entry 5, $V_{\max} = 2.39 \times 10^{-5} \text{ mol. L}^{-1} \cdot \text{min}^{-1}$, $K_{\text{cat}} = 14.34 \text{ h}^{-1}$) while those of proportion (L2/Cu: 1/1) presents a moderate catalytic activity (Table 4, entry 4, $V_{\max} = 1.14 \times 10^{-5} \text{ mol. L}^{-1} \cdot \text{min}^{-1}$, $K_{\text{cat}} = 6.84 \text{ h}^{-1}$) and those of (L2/Cu: 2/1) presents low catalytic activity (Table 4, entry 6, $V_{\max} = 0.738 \times 10^{-5} \text{ mol. L}^{-1} \cdot \text{min}^{-1}$, $K_{\text{cat}} = 4.43 \text{ h}^{-1}$ respectively) (Figure 6b).

From these results, we conclude that the associations of ligands L1 and L2 with copper acetate contribute in higher catalytic activity for *in situ* complexes. We can explain that with the nature of the acetate ion and its large size, which helps to create enough steric hindrance around the metallic center allowing the increase in the catalytic activities of the complexes [9].

Table 4 Kinetic parameters of *in situ* complexes

Entry	Complex	$10^5 V_{\max}$ (mol L ⁻¹ min ⁻¹)	$10^2 K_m$ (mol L ⁻¹)	K_{cat} (h ⁻¹)	$10^2 K_i$ (mol L ⁻¹)
1	L1[Cu(CH ₃ COO) ₂] 1:1	1.98	2.74	11.90	-
2	L1[Cu(CH ₃ COO) ₂] 1:2	7.57	1.92	45.42	4.02
3	L1[Cu(CH ₃ COO) ₂] 2:1	1.82	0.99	10.92	9.20
4	L2[Cu(CH ₃ COO) ₂] 1:1	1.14	6.65	6.84	-
5	L2[Cu(CH ₃ COO) ₂] 1:2	2.39	0.23	14.34	-
6	L2[Cu(CH ₃ COO) ₂] 2:1	0.74	3.30	4.43	-
7	L1[Co(CH ₃ COO) ₂] 1:1	22.60	0.01	135.60	0.06
8	L1[Co(CH ₃ COO) ₂] 1:2	16.40	0.15	98.40	-
9	L1[Co(CH ₃ COO) ₂] 2:1	8.95	0.35	53.70	-
10	L2[Co(CH ₃ COO) ₂] 1:1	3.32	0.90	19.92	-
11	L2[Co(CH ₃ COO) ₂] 1:2	11.80	1.03	70.80	-
12	L2[Co(CH ₃ COO) ₂] 2:1	0.40	1.10	2.43	-

**Figure 6.** Kinetic studies of the 3,5-DTBC oxidation with different concentration of copper acetate and ligands: a) L1Cu and b) L2Cu.

4.4.2. Oxidation reactions using *in situ* cobalt complexes (L1Co and L2Co)

Many transition metals were elaborated to investigate their catecholase activities such as Nickel, Zinc and cobalt [7, 12, 13]. In this work, we opted to test the catalytic capacity of *in situ* complexes of cobalt using the same ligands. *In situ* cobalt complexes were prepared in the same manner using cobalt (II) acetate.

From Figure 7a, we note that *in situ* L1Co complex (L1/Co: 1/1) follows the model of inhibition by excess of substrate at the concentration 3.10^{-2} M and applying the modified Michaelis-Menten equation (Eq. 2) (Table 4, entry 7, $V_{\max} = 22.6 \times 10^{-5}$ mol.min⁻¹L⁻¹, $K_{\text{cat}} = 135.6$). It shows highest activity (7 times) if compared to *in situ* L1Co (L1/Co: 1/2) and L1Co (L2/Co: 2/1) complexes which follows the simple Michaelis-Menten model (Eq. 1) (Table 4, entries 8 and 9, $V_{\max} = 16.4 \times 10^{-4}$ mol.min⁻¹L⁻¹, $K_{\text{cat}} = 98.4$ h⁻¹, $V_{\max} = 8.95 \times 10^{-4}$ mol.min⁻¹L⁻¹, $K_{\text{cat}} = 53.7$ h⁻¹ respectively).

For ligand L2, we note that the kinetic models of different *in situ* cobalt complexes follow the simple Michaelis-Menten equation (Eq. 1). The kinetic parameters reveal that the complex obtained from 2 moles of cobalt (II) acetate and one mole of ligand L2 exhibits the highest activity (Table 4, entry 11, $V_{\max} = 11.8 \times 10^{-5}$ mol. L⁻¹.min⁻¹, $K_{\text{cat}} = 70.8$ h⁻¹) while those of

proportion (L2/Cu: 1/1) presents good catalytic activity (Table 4, entry 10, $V_{\max} = 3.32 \times 10^{-5}$ mol. L⁻¹.min⁻¹, $K_{\text{cat}} = 19.92 \text{ h}^{-1}$) and those of (L2/Cu: 2/1) presents low catalytic activity (Table 4, entry 12, $V_{\max} = 0.404 \times 10^{-5}$ mol. L⁻¹.min⁻¹, $K_{\text{cat}} = 2.43 \text{ h}^{-1}$ respectively) (Figure 7b).

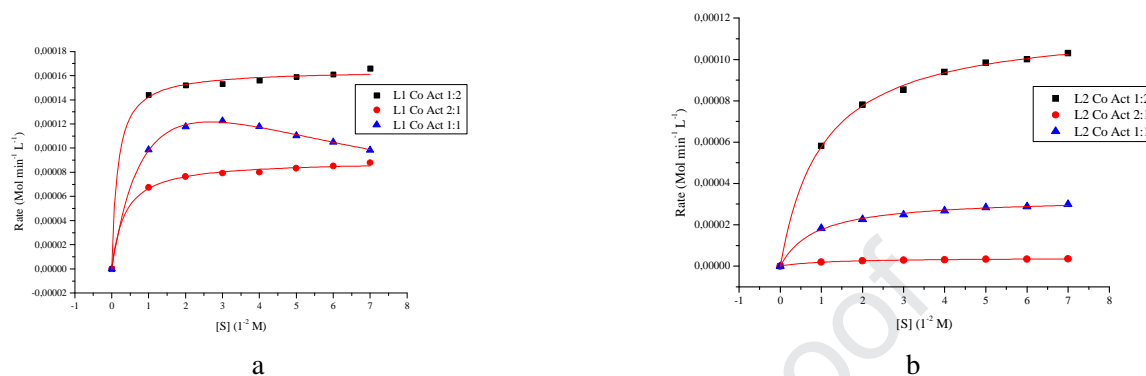


Figure 7. Kinetic studies of the 3,5-DTBC oxidation with different concentration of cobalt acetate and ligands : a) L1Co and b) L2Co.

As shown in Table 4, the difference of the catalytic activities between the two metal complexes is apparent. This is due to the nature and the electronic properties of the each metal ion. Moreover, the steric hindrance occurs between the substrate and the active site of the complex. Thus, the cobalt atomic radius is larger and it has greater oxygen affinity compared to copper atom. Furthermore, the difference in geometry of the ligands L1 and L2 have an effect on the catalytic activity. As shown in Figure 1, L1 geometry is wide which can creates more steric hindrance around the metal center. As result, the complex geometry is affected and the activity is rise [46]. In each case, the activities of cobalt complexes are more important than that of copper one (Figure 8) [12].

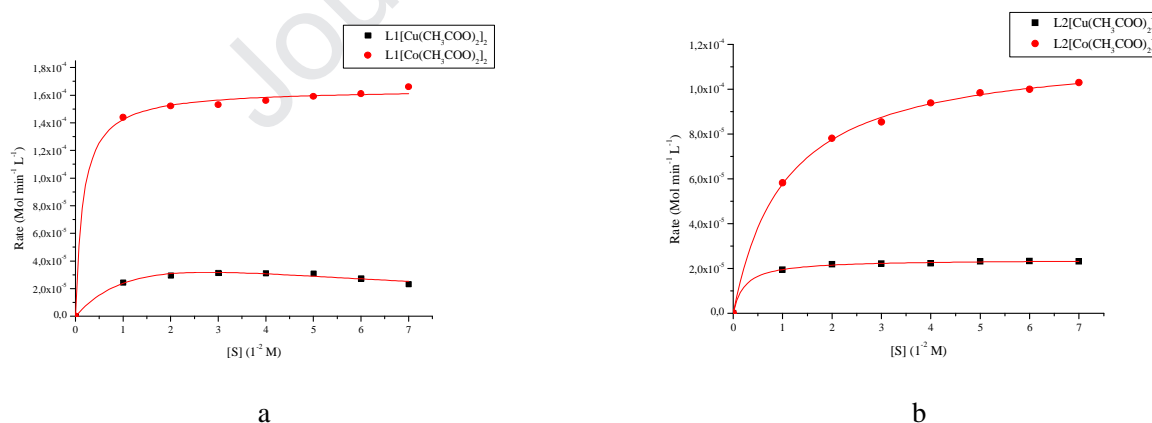


Figure 8. Kinetic studies of the 3,5-DTBC oxidation with different concentration of copper acetate and cobalt acetate and ligands: a) L1Cu / L1Co and b) L2Cu / L2Co. (L1/Co: 1/2) and (L2/Co: 1/2)

The catalytic oxidation reaction of 3,5-DTBC under the same conditions with ligands and metal salts alone was performed to evaluate their catalytic efficiency. The results show that there is low activity comparing with that of *in situ* complexes. These results are given in Table 5.

Table 5. Comparison of kinetic parameters of *in situ* complexes (copper and cobalt) with ligands (L1 and L2) and metallic salts ($\text{Cu}(\text{CH}_3\text{COO})_2$ and $\text{Co}(\text{CH}_3\text{COO})_2$).

Complex/Parameters	V_{max} ($\text{mol L}^{-1} \text{min}^{-1}$)	K_m (mol L^{-1})
L1	6.1E-6	6.72E-2
L2	Linear dependence on [S]	-
$\text{Cu}(\text{CH}_3\text{COO})_2$	6.56E-6	5.3E-2
$\text{Co}(\text{CH}_3\text{COO})_2$	1.4E-5	3.42E-2
<i>in situ</i> complex (Cu/L1:2/1)	7.57 E-5	1.92
<i>in situ</i> complex (Cu/L2:2/1)	2.39 E-5	0.23
<i>in situ</i> complex (Co/L1:2/1)	22.60 E-5	0.01
<i>in situ</i> complex Co/L2:2/1)	11.80 E-5	1.03

By comparing the catalytic efficiency of our *in situ* complexes with other results of the literature (give these results), we find that our complexes have higher maximum velocity values. We conclude that the catalytic activity of our *in situ* copper and cobalt complexes is higher compared to those prepared by Bouanane et al. And Mouadili et al [47, 48].

5. Hemolysis assay

Figures 9 show the evolution of the rate of hemolysis in percentage during the 60 min. The Ligand L1 shows an increase in hemolysis rate with concentration as a function of time (15, 30, 45, 60 min). For concentrations of 100 $\mu\text{g/mL}$ and 50 $\mu\text{g/mL}$, the rate of hemolysis increases remarkably from the first minutes until reaching 60 min, 116 % and 82 %. However for the 25 $\mu\text{g/mL}$ concentration, hemolysis only begins to evolve after 30 minutes and reaches 42 % after 60 minutes. We also find that there is no hemolysis with the concentration 12.5 $\mu\text{g/mL}$ (Figure 9a). Further, no hemolytic effect was observed with the L2 ligand whatever the concentration used (Figure 9b). We can conclude that the L1 ligand is toxic to red blood cells from the concentration 25 $\mu\text{g/mL}$, while L2 has no toxicity to red blood cells.

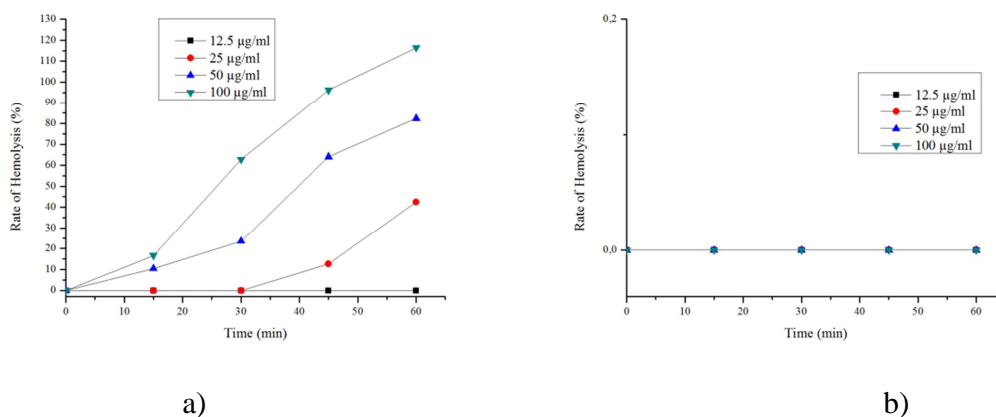


Figure 9: Evolution of the hemolysis rate as a function of time for: a) ligand L1, b) ligand L2.

6. Conclusions

Two novel thiosemicarbazone ligands L1 and L2 has been synthesized and characterized by FT-IR, ¹H NMR and mass spectroscopy analysis. L1 structure was also determined by single crystal X-ray diffraction. *In situ* catecholase activity of L1 and L2 against 3,5-DTBC was investigated with copper and cobalt transition metals. Catechol oxidation reactions were realized using different concentrations of copper and cobalt acetate and ligands (L/Cu; L/Co): 1/1, 1/2, 2/1). The oxidation reaction rates were analyzed with Michaelis-Menten equations, and the kinetic parameters were calculated. The results show that all *in situ* complexes were able to catalyze the oxidation of 3,5-DTBC. However, acetate metal salt complexes always present the highest catecholase activity. The application of the Michaelis-Menten equations revealed a difference in the mode of activity between copper and cobalt complexes. Oxidation followed by inhibition by excess of substrate concentration was applied to L1 complexes. Oxidation activation was applied to L2 complexes. The study also revealed that both the ligand structure and the metal have a major influence on the catalytic activity and model. Hemolysis tests revealed that the L1 ligand is toxic to red blood cells from the concentration 25 µg/mL, while L2 has no toxicity to red blood cells.

Supplementary Information

CCDC No. 1451400 can be obtained free of charge via <http://www.ccdc.cam.ac.uk/conts/retrieving.html>.

Acknowledgments

Authors acknowledge the Algerian Ministry for Higher Education and Research for supporting this research.

References

- [1] M. Fessenden, Illuminating life's building blocks, *Nature* 533 (2016) 565-568
- [2] E.F. Bailao, S. Lima Pde, M.G. Silva-Bailao, A.M. Bailao, R. Fernandes Gda, D.J. Kosman, C.M. Soares, *Paracoccidioides* spp. ferrous and ferric iron assimilation pathways, *Front Microbiol* 6 (2015) 821.
- [3] K.J. Waldron, J.C. Rutherford, D. Ford, N.J. Robinson, Metalloproteins and metal sensing, *Nature* 460 (2009) 823-830.
- [4] I.A. Koval, P. Gamez, C. Belle, K. Selmeczi, J. Reedijk, Synthetic models of the active site of catechol oxidase: mechanistic studies, *Chem. Soc. Rev.* 35 (2006) 814-840.
- [5] R. Marion, N.M. Saleh, N. Le Poul, D. Floner, O. Lavastre, F. Geneste, Rate enhancement of the catechol oxidase activity of a series of biomimetic monocopper(II) complexes by introduction of non-coordinating groups in N-tripodal ligands, *New J. Chem.* 36 (2012) 1828-1835.
- [6] M.I. Ayad, Synthesis, characterization and catechol oxidase biomimetic catalytic activity of cobalt(II) and copper(II) complexes containing N2O2 donor sets of imine ligands, *Arab. J. Chem* 9 (2016) 1297-1306.

- [7] S.K. Dey, A. Mukherjee, The synthesis, characterization and catecholase activity of dinuclear cobalt(II/III) complexes of an O-donor rich Schiff base ligand, *New J. Chem.* 38 (2014) 4985-4995.
- [8] R. Saddik, F. Abridach, N. Benchat, S. El Kadiri, B. Hammouti, R. Touzani, Catecholase activity investigation for pyridazinone- and thiopyridazinone-based ligands, *Res. Chem. Intermed.* 38 (2012) 1987-1998.
- [9] A. Mouadili, A. Attayibat, S.E. Kadiri, S. Radi, R. Touzani, Catecholase activity investigations using in situ copper complexes with pyrazole and pyridine based ligands, *Appl. Catal., A* 454 (2013) 93-99.
- [10] S. Sarkar, A. Sim, S. Kim, H.-I. Lee, Catecholase activity of a self-assembling dimeric Cu(II) complex with distant Cu(II) centers, *J. Mol. Catal. A: Chem.* 410 (2015) 149-159.
- [11] A. Allam, I. Dechamps-Olivier, J.-B. Behr, L. Dupont, R. Plantier-Royon, Thermodynamic, spectroscopic studies and catechol oxidase activity of copper (II) complexes with amphiphilic d-galacturonic acid derived ligands, *Inorg. Chim. Acta* 366 (2011) 310-319.
- [12] S.K. Dey, A. Mukherjee, Catechol oxidase and phenoxazinone synthase: Biomimetic functional models and mechanistic studies, *Coord. Chem. Rev.* 310 (2016) 80-115.
- [13] S. Pal, B. Chowdhury, M. Patra, M. Maji, B. Biswas, Ligand centered radical pathway in catechol oxidase activity with a trinuclear zinc-based model: synthesis, structural characterization and luminescence properties, *Spectrochim. Acta. A. Mol. Biomol. Spectrosc.* 144 (2015) 148-154.
- [14] A. El-Trass, S.Y. Shaban, Silicon (IV) complexes containing bidentate ligands; Syntheses, Characterization and Catechol oxidase activity, *Int J Adv Res* 2 (2014) 997-1006.
- [15] T. Plech, M. Wujec, A. Siwek, U. Kosikowska, A. Malm, Synthesis and antimicrobial activity of thiosemicarbazides, s-triazoles and their Mannich bases bearing 3-chlorophenyl moiety, *Eur. J. Med. Chem.* 46 (2011) 241-248.
- [16] S.N. Pandeya, D. Sriram, G. Nath, E. DeClercq, Synthesis, antibacterial, antifungal and anti-HIV activities of Schiff and Mannich bases derived from isatin derivatives and N-[4-(49-chlorophenyl)thiazol-2-yl] thiosemicarbazide, *Eur. J. Pharm. Sci.* 9 (1999) 25-31.
- [17] E. Palaska, G.I. Sahin, P. Kelicen, N.T.b. Durlu, G.I.i. Altinok, Synthesis and anti-inflammatory activity of 1-acylthiosemicarbazides, 1,3,4-oxadiazoles, 1,3,4-thiadiazoles and 1,2,4-triazole-3-thiones, *Il Farmaco* 57 (2002) 101-107.
- [18] G. Kucukguzel, A. Kocatepe, E. De Clercq, F. Sahin, M. Gulluce, Synthesis and biological activity of 4-thiazolidinones, thiosemicarbazides derived from diflunisal hydrazide, *Eur. J. Med. Chem.* 41 (2006) 353-359.
- [19] J.F. de Oliveira, A.L. da Silva, D.B. Vendramini-Costa, C.A. da Cruz Amorim, J.F. Campos, A.G. Ribeiro, R. Olimpio de Moura, J.L. Neves, A.L. Ruiz, J. Ernesto de Carvalho, C. Alves de Lima Mdo, Synthesis of thiophene-thiosemicarbazone derivatives and evaluation of their in vitro and in vivo antitumor activities, *Eur. J. Med. Chem.* 104 (2015) 148-156.
- [20] E.C. Moore, Morris S. Zedeck, K.C. Agrawal, A.C. Sartorelli, Inhibition of ribonucleoside diphosphate reductase by 1-formylisoquinoline thiosemicarbazone and related compounds., *Biochemistry (Mosc.)* 9 (1970) 4492-4498.

- [21] R. Manikandan, P. Anitha, G. Prakash, P. Vijayan, P. Viswanathamurthi, R.J. Butcher, J.G. Malecki, Ruthenium(II) carbonyl complexes containing pyridoxal thiosemicarbazone and trans-bis(triphenylphosphine/arsine): Synthesis, structure and their recyclable catalysis of nitriles to amides and synthesis of imidazolines, *J. Mol. Catal. A: Chem.* 398 (2015) 312-324.
- [22] M. Mohamed Subarkhan, R. Ramesh, Binuclear ruthenium(III) bis(thiosemicarbazone) complexes: synthesis, spectral, electrochemical studies and catalytic oxidation of alcohol, *Spectrochim. Acta. A. Mol. Biomol. Spectrosc.* 138 (2015) 264-270.
- [23] D.J. Hayne, S. Lim, P.S. Donnelly, Metal complexes designed to bind to amyloid-b for the diagnosis and treatment of Alzheimer's disease, *Chem. Soc. Rev.* 43 (2014) 6701-6715.
- [24] S. Lim, B.M. Paterson, M.T. Fodero-Tavoletti, G.J. O'Keefe, R. Cappai, K.J. Barnham, V.L. Villemagne, P.S. Donnelly, A copper radiopharmaceutical for diagnostic imaging of Alzheimer's disease: a bis(thiosemicarbazone)copper(II) complex that binds to amyloid-beta plaques, *Chem Commun.* 46 (2010) 5437-9.
- [25] J.M. Cano Pavon, J.C. Jimenez Sanchez, F. Pino, The 4-phenyl-3-thiosemicarbazone of biacetylmonoxime as an analytical reagent. spectrophotometric determination of manganese, *Anal. Chim. Acta* 75 (1975) 335-342.
- [26] R.B. Singh, B.S. Garg, R.P. Singh, Analytical applications of thiosemicarbazones and semicarbazones: A review, *Talanta* 25 (1978) 619-632.
- [27] A.S. Fouda, M.N. Moussa, F.I. Taha, A.I. Eleneanaa, The role of some thiosemicarbazide derivatives in the corrosion inhibition of aluminium in hydrochloric acid, *Corros. Sci.* 26 (1986) 719-726.
- [28] B. Houari, S. Louhibi, K. Tizaoui, L. Boukli-hacene, B. Benguella, T. Roisnel, V. Dorcet, New synthetic material removing heavy metals from aqueous solutions and wastewater, *Arab. J. Chem* (2016).
- [29] A. Altomare, M.C. Burla, M. Camalli, G.L. Casciarano, C. Giacovazzo, A. Guagliardi, A.G.G. Moliterni, G. Polidori, R. Spagna, SIR97: a new tool for crystal structure determination and refinement, *J. Appl. Crystallogr.* 92 (1999) 115-119.
- [30] G.M. Sheldrick, A short history of SHELX, *Acta Crystallographica Section A* 64 (2008) 112-122.
- [31] W. Lee, Y. Kim, J. Lim, M. Kim, E.J. Lee, A. Lee, K.Y. Lee, C.S. Kang, S.Y. Kim, K. Han, S.H. Pai, Rapid, sensitive diagnosis of hemolytic anemia using antihemoglobin antibody in hypotonic solution, *Ann. Clin. Lab. Sci.* 32 (2002) 37-43.
- [32] K. Alomar, A. Landreau, M. Kempf, M.A. Khan, M. Allain, G. Bouet, Synthesis, crystal structure, characterization of zinc(II), cadmium(II) complexes with 3-thiophene aldehyde thiosemicarbazone (3TTSCH). Biological activities of 3TTSCH and its complexes, *J. Inorg. Biochem.* 104 (2010) 397-404.
- [33] I. Pal, F. Basuli, S. Bhattacharya, Thiosemicarbazone complexes of the platinum metals. A story of variable coordination modes, *J. Chem. Sci.* 114 (2002) 255-268.
- [34] C.F. Bell, K.A.K. Lott, N. Hearn, Copper complexes of pyridine 2-aldehyde and 2-acetylpyridine thiosemicarbazones, *Polyhedron* 6 (1987) 39-44.

- [35] X.Y. Jiang, L.Q. Sheng, C.F. Song, N.Na Du, H.J. Xu, Z. Liu, and S.S. Chen, Mechanism, kinetics, and antimicrobial activities of 2-hydroxy-1-naphthaldehyde semicarbazone as a new jack bean urease inhibitor, *New J. Chem.* 40 (2016) 3520-3527.
- [36] H. Beraldo, R. Lima, L.R. Teixeira, A.A. Moura, D.X. West, Crystal structures and IR, NMR and UV spectra of 4-formyl- and 4-acetylpyridine N(4)-methyl- and N(4)-ethylthiosemicarbazones, *J. Mol. Struct.* 559 (2001) 99-106.
- [37] I.C. Mendes, L.R. Teixeira, R. Lima, H. Beraldo, N.L. Speziali, D.X. Westc, Structural and spectral studies of thiosemicarbazones derived from 3- and 4-formylpyridine and 3- and 4-acetylpyridine, *J. Mol. Struct.* 559 (2001) 355-360.
- [38] D.-H. Wu, C. He, C.-Y. Duan, X.-Z. You, Terephthalaldehyde bis(thiosemicarbazone) bis(dimethylformamide) solvate, *Acta Crystallographica Section C* C56 (2000) 1336-1337.
- [39] B. Houari, S. Louhibi, L. Boukli-Hacene, T. Roisnel, M. Taleb, (E)-2-[(1H-Imidazol-4-yl)methyl-ylene]hydrazinecarbo-thio-amide monohydrate, *Acta Cryst. E* 69 (2013) 1469.
- [40] A. Çukurovali, I. Yilmaz, H. Özmen, M. Ahmedzade, Cobalt(II), copper(II) nickel(II) and zinc(II) complexes of two novel Schiff base ligands and their antimicrobial activity, *Transit. Met. Chem.* 27 (2002) 171-176.
- [41] D.A. Paixão, L.P. de Oliveira, P.I. da S. Maia, V.M. Deflon, Z.A. Carneiro, K.J. de Almeida, N.P. Lopes, M. Pivatto, J.D.S. Chaves, S. de Albuquerque, M.V. de Almeida, S. Guilardi, W. Guerra, Crystal structure of two new polymeric copper(II) complexes active against *Trypanosoma cruzi*, *Journal of Saudi Chemical Society* 22 (2018) 809-815.
- [42] B. Chiari, A. Cinti, O. Crispu, F. Demartin, A. Pasini, O. Piovesana, New pentanuclear mixed valence Co(II)-Co(III) complexes of "short" salen homologues, *J. Chem. Soc., Dalton Trans.*, 24 (2002) 4672-4677.
- [43] N. Kitajima, K. Fujisawa, Y. Morooka, K. Toriumi, .mu.-eta.2:.eta.2-Peroxo binuclear copper complex, [Cu(HB(3,5-(Me₂CH)₂pz)₃)]₂(O₂), *J. Am. Chem. Soc.* 111 (1989) 8975-8976.
- [44] W.M. Singh, T. Baine, S. Kudo, S. Tian, X.A. Ma, H. Zhou, N.J. DeYonker, T.C. Pham, J.C. Bollinger, D.L. Baker, B. Yan, C.E. Webster, X. Zhao, Electrocatalytic and photocatalytic hydrogen production in aqueous solution by a molecular cobalt complex, *Angew. Chem. Int. Ed. Engl.* 51 (2012) 5941-4.
- [45] Inorganic chemistry 1995 O. Schlager, K. Wieghardt, and B. Nuber, Trivalent transition metal complexes [M^{III}(L-3H)] (M = Fe, Co,) of the triply deprotonated hexadentate ligand 1,4,7-tris(*o*-aminobenzyl)-1,4,7-triazacyclononane (L). Crystal structure of [Mn^{IV}(L-3H)]BPh₄, *Inorg. Chem.*, 34 (1995) 6456-6462.
- [46] N. Boussalah, R. Touzani, I. Bouabdallah, S.E. Kadiri, S. Ghalem, Synthesis, structure and catalytic properties of tripodal amino-acid derivatized pyrazole-based ligands, *J. Mol. Catal. A: Chem.* 306 (2009) 113-117.
- [47] R. Boyaala, R. El Ati, M. Khoutoul, M. El Kodadi, R. Touzani, B. Hammouti, Biomimetic oxidation of catechol employing complexes formed in situ with heterocyclic ligands and different copper(II) salts, *IRAN CHEM SOC*, 15 (2017) 1-8.
- [48] A. Mouadili, F.F. Al-blewi, N. Rezki, M. Messali, A. El Ouafi, R. Touzani, Biomimetic catecholase studies: using in-situ prepared complexes by 1,2,4-triazole schiff bases and different metal salts, *J. Mater. Environ. Sci.*, 6 (2015) 2392-2399.

[48] Moualidi et al.

Journal Pre-proof

Highlights

- Synthesis of new thiosemicarbazone derivative L1 and L2 ligands
- Crystal structure of L1
- Copper and Cobalt *in situ* complexes catecholase activity
- *In situ* complexes of L1 act as catalysts and inhibitors
- *In situ* complexes of L2 act as a catalysts
- Hemolytic activity

Author Contribution Statement

Ousama Nehar: realization of all the experimental part (except hemolysis), tracet graphs, interpretation, validation of results, writing and correction of a part of the article.

Radia Mahboub: interpretation of part of the results and correction of the writing.

Samira Louhibi: Interpreting the results, writing and correcting the writing of part of the article.

Thierry Roisnel: Single crystal study

Mohammed Aissaoui: Writing and realization of the experimental hemolysis partwriting and correction of a part of the article.

Declaration of interests

The authors declare that they have no known competing financial interests or personal relationships that could have appeared to influence the work reported in this paper.

The authors declare the following financial interests/personal relationships which may be considered as potential competing interests: